Supplemental Methods

Array Comparative Genomic Hybridization (aCGH). In brief, 300 ng of sample and reference DNA from pre-treatment prostate biopsies were differentially labeled in a random priming reaction with Cyanine 3–dCTP and Cyanine 5–dCTP (Perkin Elmer Life Sciences). DNA samples were then combined and mixed with 100 µg of human Cot-1 DNA (Invitrogen) followed by removal of unincorporated nucleotides using microcon YM-30 columns (Millipore). Sample mixtures were denatured at 85°C for 10 min, and repetitive sequences were blocked at 45°C for 1 hr before hybridization. The mixture was then applied onto arrays containing 26,819 bacterial artificial chromosome (BAC) derived amplified fragment pools spotted in duplicate on aldehyde coated glass slides (SMRT v.2, BC Cancer Research Centre Array Facility). Array hybridization was performed in the dark at 45°C for 36 hr inside a hybridization chamber, rinsed four times in 0.1X SSC at room temperature and dried by centrifugation at 1,000g before imaging. Slides were scanned using a dual laser array scanner (Axon) and spot signal intensities determined using the SoftWoRx Tracker Spot Analysis software (Applied Precision). The log2 ratios of the Cyanine 3 to Cyanine 5 intensities for each spot were assessed. Data was then normalized using a stepwise normalization procedure (5). Regions of copy number alterations were identified via data visualization using SeeGH software (available at http://www.flintbox.ca/technology) and loss, normal, and gain probabilities for each clone as determined by a modified Hidden Markov Model. Data were filtered and normalized (65) based on both replicate standard deviation (data points with greater than 0.075 standard deviation removed) and signal to noise ratio (data points with a signal to noise ratio less than 10 removed). The genomic positions of clones were mapped to the UCSC Genome Browser April 2003.

Statistical Analysis. For clinical data analyses, aberrant CGH regions were identified with smoothing prior to statistical analyses using an HMMer algorithm (66). The number of hedgehog gene abnormalities in a given patient was determined by calculating the total number of losses and gains for each of the following hedgehog genes: PTCH1, GLI1, GLI2, GLI3, SMO, MMP9, SHH, IHH, DHH, SNAI1, SNAI2, SNAI3, CYCLIN D1, SERPIN2, and SMAD9. A patient was considered to have a hedgehog abnormality if he had either a gain or a loss in any of region of PTCH1, GLI1, GLI2, GLI3, SMO, MMP9, SHH, IHH, DHH, SNAI1, SNAI2, SNAI3, or CYCLIN D1, or a loss in SMAD9 or gain in PN1. A patient was considered to have a hedgehog abnormality if he had either a gain or a loss in any region within the particular gene of interest. Gains or losses in a particular region were called using a robust hidden Markov model (HMM). The percentage of entire genome alteration (PGA) was calculated as the total number of altered base pairs divided by the total number of base pairs in the human genome. Relapse-free rate (RFR) was calculated as the time from the start of radio- or neo-adjuvant hormone-therapy to the date of biochemical relapse (as determined by the Phoenix definition whereby failure is defined as any post-treatment PSA greater than the nadir PSA value plus 2.0ng/ml) or the date of last PSA measurement. Univariate associations with RFR were investigated with the Kaplan-Meier method and the log-rank test. Cox proportional hazards regression models were fit to assess the independent prognostic ability of having 2 or more hedgehog gene abnormalities compared with one or less, adjusting for the effect of PGA, T-category, pre-treatment PSA, and Gleason score. T-category and Gleason Score were modelled as categorical variables (T1 vs T2 and 6 vs 7 respectively), while PGA and PSA were modelled as continuous variables in all analyses. In this intermediate risk group of 126 patients, there were 47 biochemical relapses, 42 of which met the Phoenix definition for failure, and an additional five that were pre-emptively treated with salvage hormones by their physician due to a rising PSA. Fisher's exact tests were used to investigate the relationship between PTEN or TMPRSS2-ERG fusion and the number of hedgehog gene alterations. Mann-Whitney-Wilcoxon tests were used to compare PGA between those patients with one or fewer hedgehog alterations and those patients with more than two alterations. All clinical statistical analyses were completed using R software and a p-value of 0.05 was used to assess significance of all statistical tests.

References

65. Khojasteh, M., Lam, W.L., Ward, R.K., and MacAulay, C. 2005. A stepwise framework for the normalization of array CGH data. *BMC bioinformatics* 6:274.

66. Shah, S.P., Xuan, X., DeLeeuw, R.J., Khojasteh, M., Lam, W.L., Ng, R., and Murphy, K.P. 2006. Integrating copy number polymorphisms into array CGH analysis using a robust HMM. *Bioinformatics* 22:e431-439.

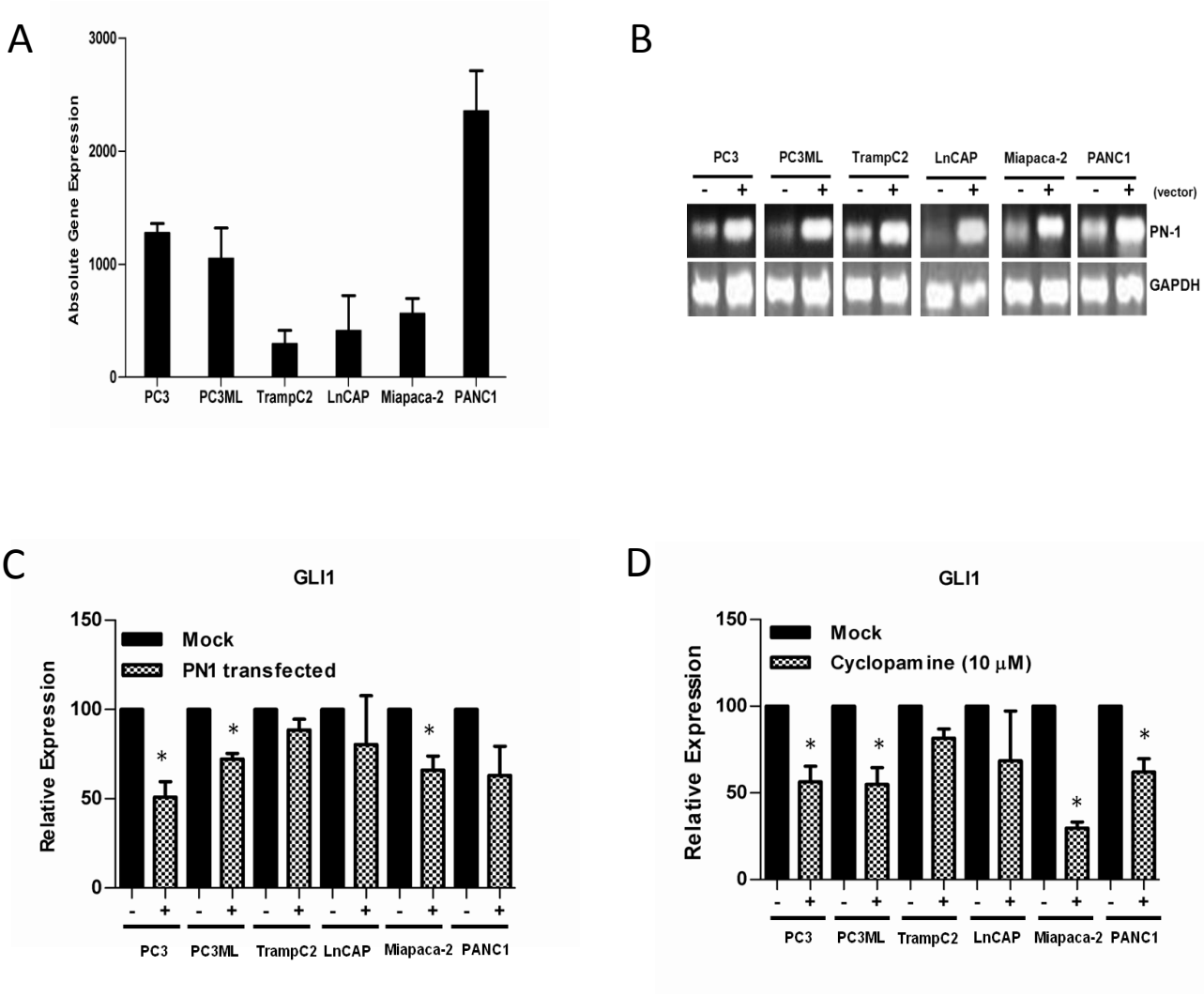

Supplemental Figure 1.

Expression of PN1 in prostate and pancreatic cancer cells**. (A)** RT-PCR of RNA transcripts reveal that PN1 is basally expressed in all prostate (PC3, PC3ML, TrampC2, LNCAP) and pancreas cell lines (Miapaca, PANC1) tested. **(B)** Amplification of PN1 levels is possible using a transfected PN1 expression vector (2μM) in all cell lines. RT-PCR amplification products were run on 1.5% high resolution gels to confirm cycle threshold (CT) levels. **(C)** RT-PCR of RNA transcripts from each cell line was tested for changes of GLI1 levels following PN1 expression. Significant decreases were observed in the transcripts of PC3, PC3ML, Miapaca-2, and PANC1. Statistical significance was determined using the Student's T-Test and denoted as * ($p \leq .05$, n=4). **(D)** Each member of the prostate/pancreatic cell line panel was also tested for their respective response to the Hh inhibitor cyclopamine, using GLI1 as a read-out. Significant decreases were observed in the transcripts of PC3, PC3mL, and Miapaca-2. Statistical significance was determined using the Student's T-Test and is denoted as * ($p \leq .05$, n=4). RNA transcripts normalized against GAPDH.

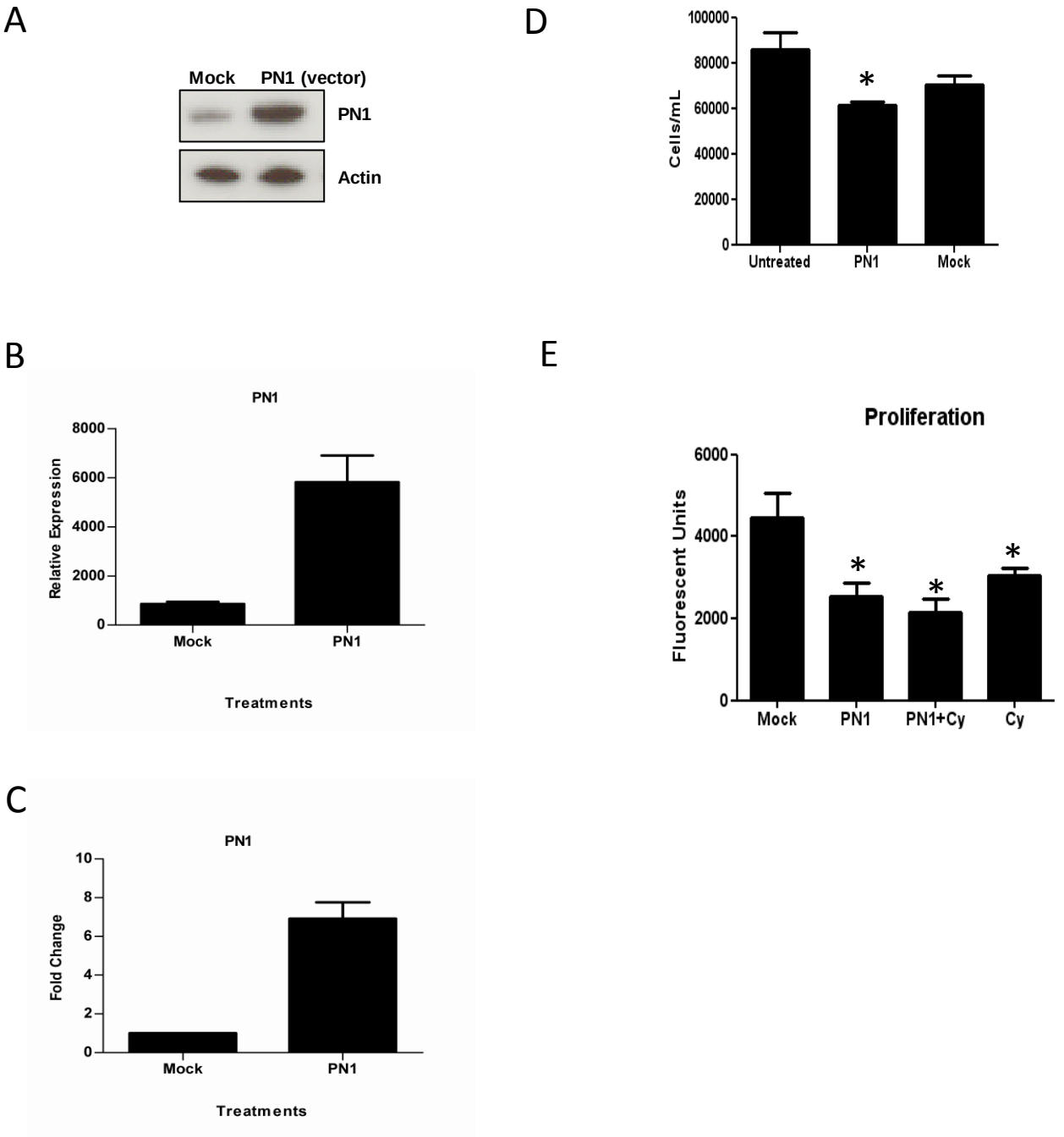

Supplemental Figure 2.

PN1 protein expression in PC3 and TrampC2 cells**. (A)** Western blot of protein levels using an empty vector or PN1 transfection vector (2µM) after 48 hr in PC3 cells. **(B)** Quantitation of relative protein expression after empty vector and PN1 transfection and **(C)** relative fold changes after treatment with PN1 expression vector in PC3 cells. Statistical significance was determined using Student's T-Test and denoted as * (p≤ .05, n=3). **(D)** PN1 transfection of TrampC2 cells leads to a reduction in cell division. Statistical significance was determined using the Student's T-Test and significance is denoted as * (p≤ .05, n=4). **(E)** Expression of PN1, alone or in combination with cyclopamine (10µM), reduces proliferation of TrampC2 cells using an Alamar Blue assay. Statistical significance was determined using a One-Way ANOVA and denoted as * (p≤ .05, n=4).

A

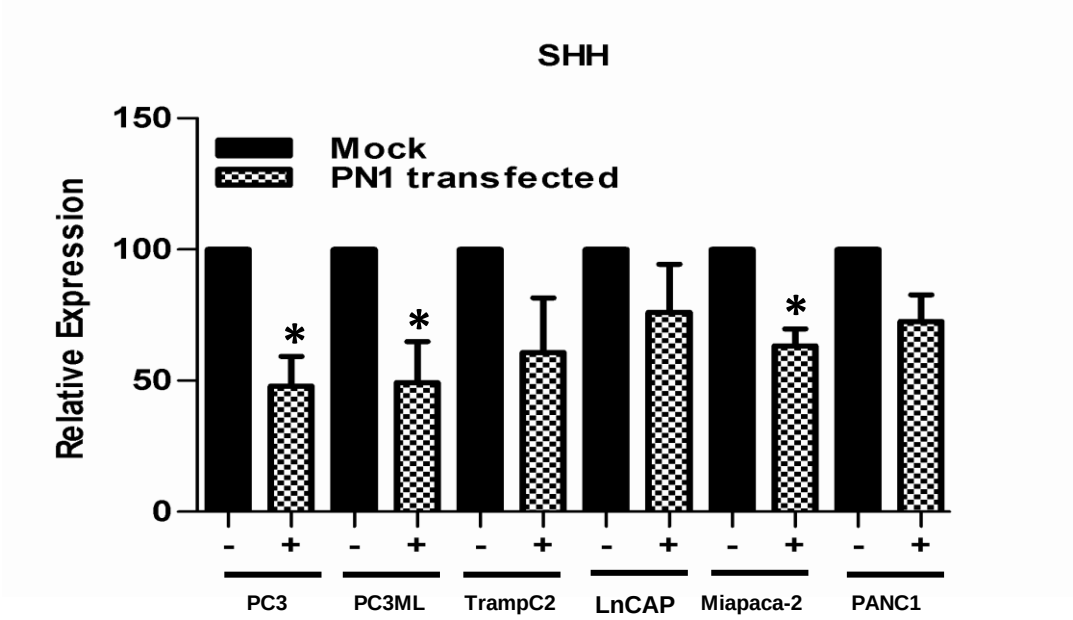

B

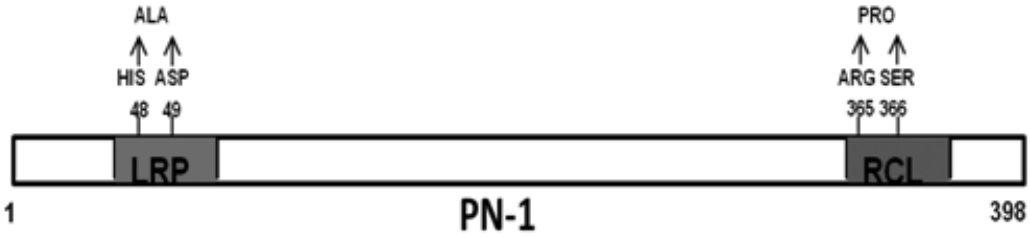

C

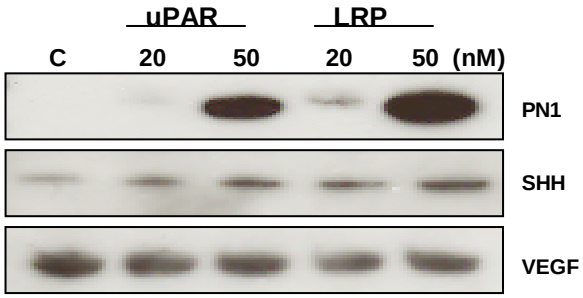

Supplemental Figure 3

Expression of SHH in prostate and pancreatic cancer cells. **(A)** RT-PCR of RNA transcripts from each cell line was tested for changes in SHH following PN1 expression. Significant decreases were observed in the transcripts of PC3, PC3mL, and Miapaca-2. RNA transcripts normalized against GAPDH. Statistical significance was determined using Student's T-Test. Statistical significance is denoted as * ($p \leq .05$, n=4). **(B)** Mutation scheme devised to inhibit the function of the LRP-1 binding site or the RCL, the site of PN1 protease activity. **(C)** Use of anti-uPAR and anti-LRP neutralizing antibodies (20 or 50 nM) in the concentrated medium of PC3 leads to increases in extracellular PN1 and SHH. VEGF used as a loading control.

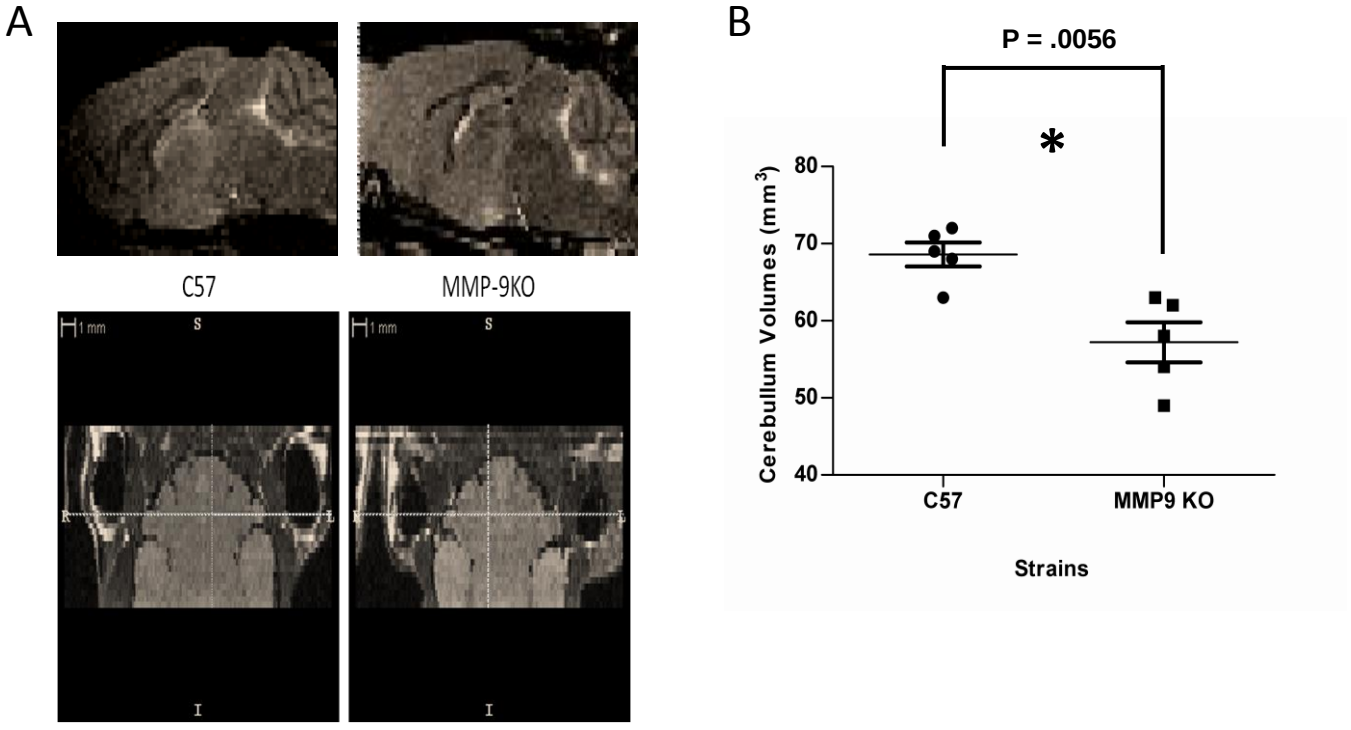

Supplemental Figure 4

Ablation of MMP-9 leads to decreased cerebella size. **(A)** Sagittal and axial views of WT and *MMP9-/-* mouse cerebella. **(B)** Comparison of brains between WT and *MMP9-/-* showed that absence of MMP9 resulted in overall smaller cerebella at comparable ages. Statistical significance was determined using Student's T-Test. Statistical significance is denoted as * (p≤ .05, n=5). **(C)** Comparison of brain volumes between WT and *MMP9-/-* showed that cerebella/total brain ratios was greater for WT than *MMP9 KO*. Statistical significance was determined using Student's T-Test. Statistical significance is denoted as * (p≤ .05, n=5). **(D)** Comparison of total brain volume between WT and *MMP9-/-* showed no significant difference. No Statistical significance (NS) was determined using Student's T-Test (n=5).

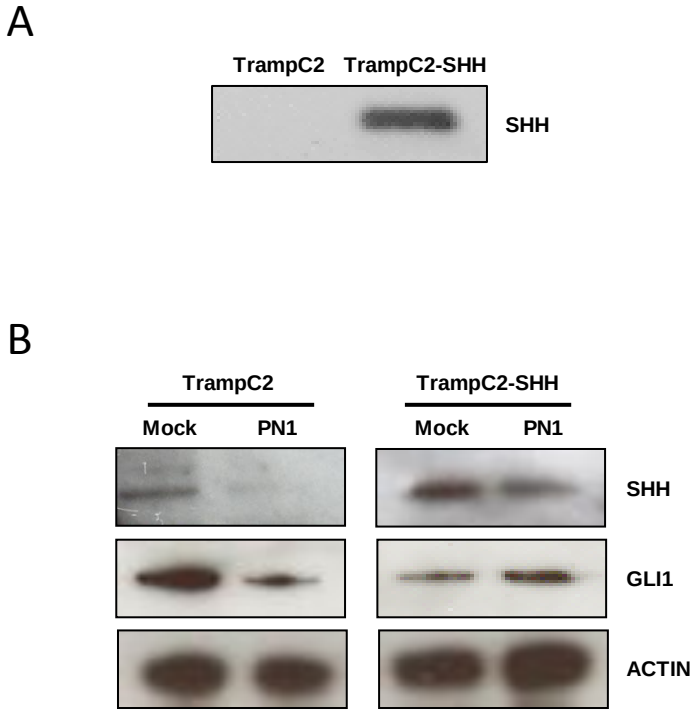

Supplemental Figure 5

SHH accelerates orthotopic tumor growth. **(A)** Stable expression of SHH at day 17 from pooled TrampC2-SHH cells. **(B)** Comparison of SHH and GLI expression in the presence of PN1 vector (2 μM) in TrampC2 cells (left) and TrampC2-SHH cells (right). TrampC2-SHH cells maintain SHH and GLI1 levels despite PN1 co-over-expression.

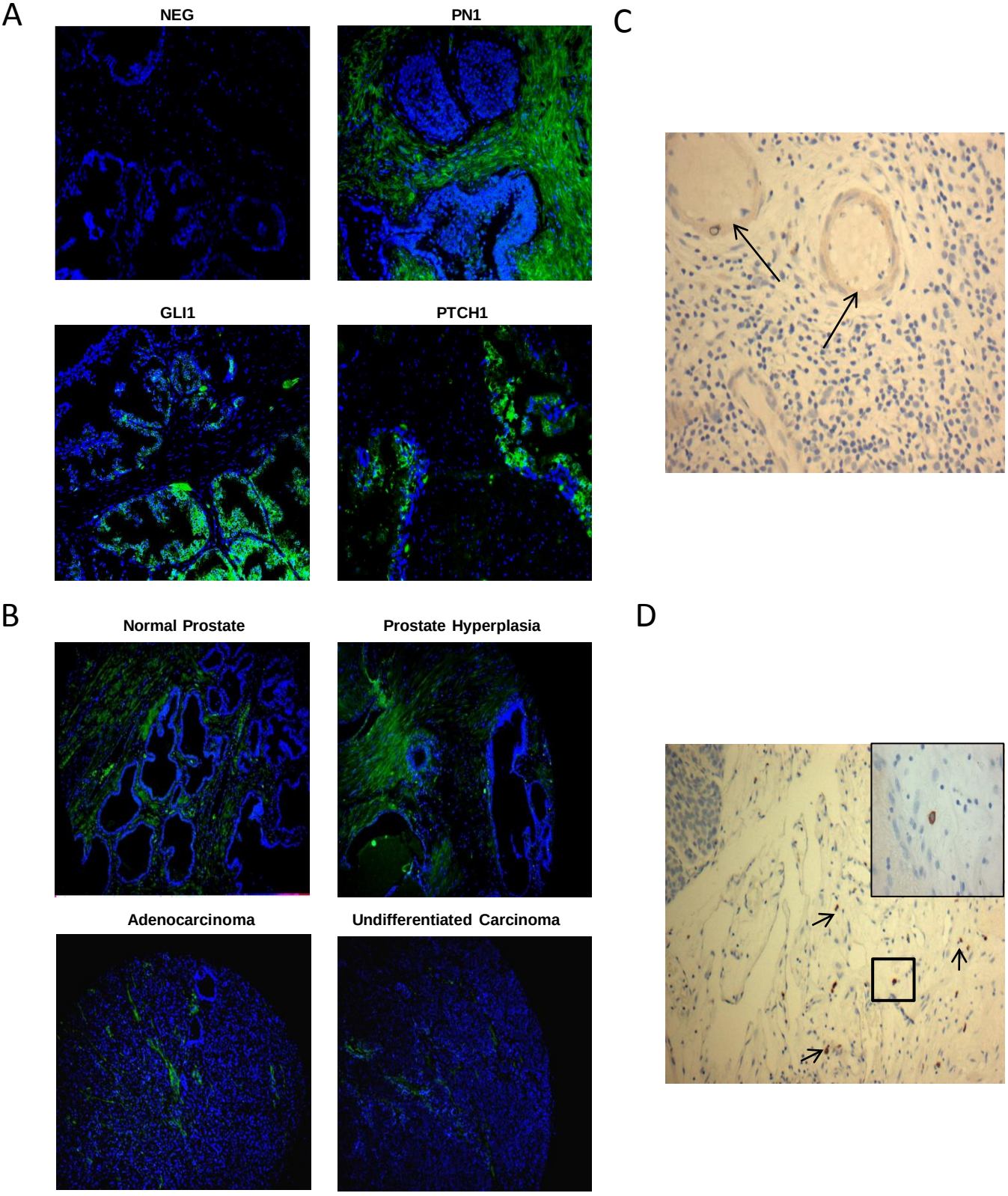

Supplemental Figure 6

Expression of PN1 and Hh Proteins in human cancer cells. **(A)** Distribution of Hh proteins in human prostate using immunofluorescence. Expression of PN1 was limited to the stroma, whilst GLI1 and PTCH1 were specific to epithelial cells in human tumor tissue. Green stain represents positive PN1 stain and nuclei is stained blue. The no-primary control was clean of all stain. **(B)** Normal prostate and hyperplasia expressed PN1 most commonly in the stroma. In tumor cells little staining was seen within the fibrous bands inside the body of the tumor and in some cases some staining appeared within the tumor cells. Normal prostate tissue expressed PN1 primarily in the stromal compartments although stain is also present in blood vessels (long arrows) **(C)** and in the cytoplasm of some stromal cells (short arrows) **(D)**.

A

	Amplifications	Deletions
PTCH1	3	1
GLI1	1	0
GLI2	3	14
SMO	9	1
MMP9	6	0
SHH	16	2
IHH	1	1
DHH	2	0
SNAI1	7	0
SNAI2	8	4
SNAI3	3	21
CyclinD1	7	1
SERPIN2 (PN1)	1	1
GLI3	9	0

B

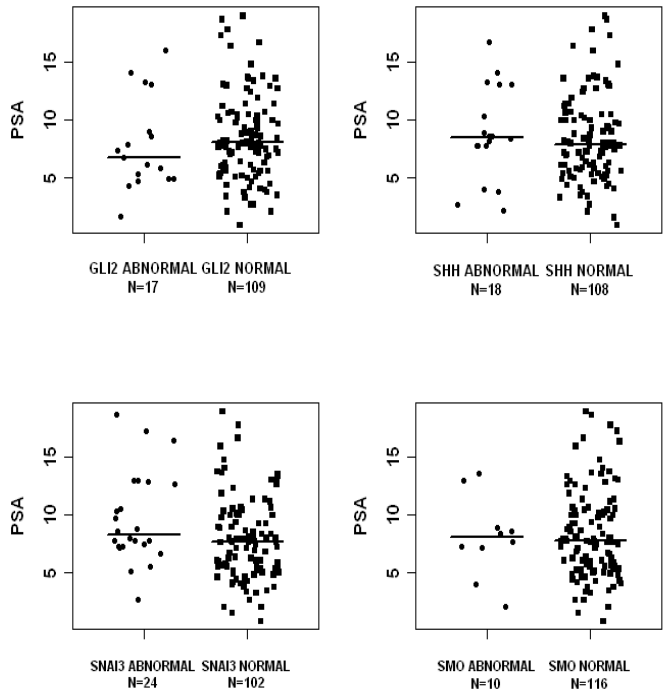

C

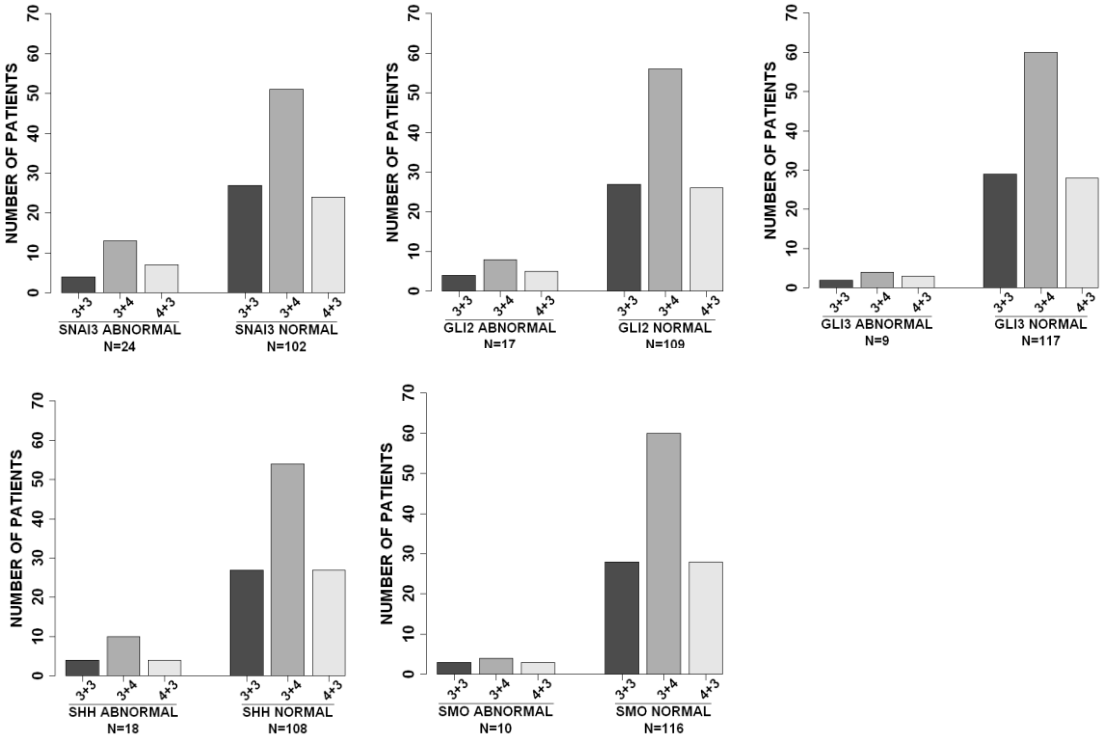

Supplemental Figure 7

Impact of Hh genetic changes in relation to PSA and Gleason 6-7 tumours. **(A)** Genes of interest exhibiting copy number alteration (CNA; amplification or deletion) in patients (N=126) presenting with intermediate risk adenocarcinoma. **(B)** Comparison of PSA levels in patients who are without or with at least one mutation in Hh genes GLI2, SHH, SMO, or SNAI. **(C)** Comparison of patients who are without or with at least one mutation in Hh genes GLI2, SHH, SMO, or SNAI and also are pathologically evaluated as Gleason 6 or 7.

Cerebellum Size

C57/B6

Animal	Animal Wt.	Cerebellum Volume (mm^3)
C57/B6 1	25	71
C57/B6 2	26	69
C57/B6 3	26	63
C57/B6 4	28	68
C57/B6 5	26	72

Avg. cerebellum vol.: 68.6 mm^3

MMP9 KO

Animal	Animal Wt.	Cerebellum Volume (mm^3)
MMP9KO 1	28	49
MMP9KO 2	27	58
MMP9KO 3	27	54
MMP9KO 4	28	62
MMP9KO 5	28	63

Avg. cerebellum vol.: 57.2 mm^3

Supplemental Table 1
Cerebellum sizes of C57 wild type mice compared to MMP9 KO mice.

Intraprostate Tumors

C57/B6

%tumor: 7/9 (78%)

Animal	Animal Wt.	Tumor volume (mm^3)
C57/B6 1	25	N/A
C57/B6 2	26	304
C57/B6 3	26	127
C57/B6 4	28	138
C57/B6 5	26	169
C57/B6 6	27	227
C57/B6 7	26	125
C57/B6 8	26	45
C57/B6 9	27	N/A

Avg. tumor vol.: 162mm^3

MMP-9 KO

%tumor: 4/10 (40%)

Animal	Animal Wt.	Tumor Volume (mm^3)
MMP9KO 1	28	N/A
MMP9KO 2	27	N/A
MMP9KO 3	27	N/A
MMP9KO 4	28	133
MMP9KO 5	28	N/A
MMP9KO 6	27	N/A
MMP9KO 7	28	N/A
MMP9KO 8	29	109
MMP9KO 9	30	60
MMP9KO 10	30	134

Avg. tumor vol.: 109 mm^3

Supplemental Table 2
Tumour sizes of C57 wild type mice compared to MMP9 KO mice following intraprostatic injection.

Intraprostate Tumors

C57/B6

%tumor: 1/5 (20%)

Animal	Animal Wt.	Tumor volume (mm^3)
C57/B6 1	23	53
C57/B6 2	25	N/A
C57/B6 3	20	N/A
C57/B6 4	20	N/A
C57/B6 5	19	N/A

PN1 KO

%tumour: 4/5 (80%)

Animal	Animal Wt.	Tumor Volume (mm^3)
PN1 KO 1	20	73
PN1 KO 2	22	60
PN1 KO 3	19	63
PN1 KO 4	23	213
PN1 KO 5	23	N/A

Supplemental Table 3
Tumour sizes of C57 wild type mice compared to PN1 KO mice following intraprostatic injection.

Strains	Fold Change	p-value
WT vs. WT+SHH	1.53	0.0284
WT vs. PN1 KO	1.80	0.0436
WT vs. PN1 KO+SHH	2.10	0.0144
WT vs. MMP9 KO	0.60	0.0211
WT vs. MMP9 KO+SHH	1.04	0.5280

Supplemental Table 4. Prostate tumor growth comparisons. Respective knockout mice with or without SHH over-expression compared to their respective C57 control groups. Fold changes are listed and deemed significant if ($p \leq .05$) using a Student's T-Test.

Variable	Hazard Ratio	95% CI		p-value
Number of Genes Altered (2+ vs 0/1)	3.046	1.362	6.815	0.0067
PGA	1.025	0.982	1.069	0.26
PSA (continuous)	1.133	1.051	1.222	0.0011
Stage (T1 vs T2)	1.213	0.646	2.281	0.55
Gleason Score (6 vs 7)	0.905	0.45	1.82	0.78

Supplmental Table 5. Multivariate analysis showing increased CNAs of Hh genes. Pre-treatment prostate-specific antigen (PSA) are independent prognostic factors for biochemical relapse in a model also containing percentage of genomic alteration (PGA), T-category, and Gleason score.

	PTEN Normal	PTEN Abnormal	Total
0/1 Genes Altered	81 (89.0%)	10 (11.0%)	91
2+ Altered	26 (74.3%)	9 (25.7%)	35
Total	107	19	126

Supplementary Table 6. Correlation of PTEN deletion with patients who presenting with two or more Hh CNAs; Fisher's test p-value≤ .05.

	Normal	TMPRSS2:ERG Fusion	Total
0/1 Genes Altered	73 (80.2%)	18 (19.8%)	91
2+ Altered	22 (62.9%)	13 (37.1%)	35
Total	95	31	126

Supplementary Table 7. Correlation of TMPRSS2:ERG fusion with patients who presenting with two or more Hh CNAs; Fisher's test p-value =.06.

Gene	Forward	Reverse
PN-1 (human)	5'GAAGCAAGCTCGCCATGGT3'	5'AGACGATGGCCTTGTTGATC3'
PN-1 (mouse)	5'AATCACAAATCAGGCTCCTA3'	5'GAGAGTCCAGAGCGTTACAC3'
GLI1 (human)	5'AGGCTCAGCTTGTGTGTAAT3'	5'AGGAACCTGACTTGTGATTG3'
GLI1 (mouse)	5'GCGATATAATGTAAACGGAG3'	5'CAAAAATTGATGGACTCAGAG3'
SHH	5'CAGCGACTTCCTCACTTTCC3'	5'GGAGCGGTTAGGGCTACTCT3'
CyclinD1	5'GGCACCTGGATTGTTCTGTT'	5'CAGCTTGCTAGGGAACTTGG3'
PTCH1	5'TTTGGACTGCTTCCTGGGAAGGG3'	5'TTTTTGTTGGGGCTGTGGC3'
GAPDH	5'CCACCCATGGCAAATTCCATGGCA3'	5'TCTAGACGGCAGGTCAGGTCCACC3'

Primer Table
All primers used for RT-PCR experiments.